REVIEW ARTICLE

Description of Different Phases of Brain Tumor Classification

Sudipta Roy[1], Samir Kumar Bandyopadhyay[2]

[1]Department of Computer Science and Engineering, Institute of Computer Technology (UVPCE), Ganpat University, Ahmadabad, Gujarat, India, [2]Department of Computer Science and Engineering, JIS University, Kolkata, West Bengal, India

ABSTRACT

The proposed approach makes contributions in various stages in the development of a computer-aided diagnosis (CAD) system of brain diseases, namely image preprocessing, intermediate processing, detection, segmentation, feature extraction, and classification. Literature study incorporates many important ideas for abnormalities detection and analysis with their advantages and disadvantages. Literature studies have pointed out the needs of dividing task and appropriate ways for accurate abnormality characterization to provide a proper clinical diagnosis.

Key words: Brain tumor, classification, pre-processing, segmentation, textural feature extraction

INTRODUCTION

Brain tumor, stroke, hemorrhage, and multiple sclerosis (MS) disease are the life-threatening diseases in both male and female. A brain tumor is the most common and widespread disease among these brain diseases. The worldwide cancer incidence of brain tumor is 3.4/100,000 people (men: 3.9/100,000 and women: 3.0/100,000). A total of 256,213 affected worldwide (139,608 men and 116,605 women). The trend of new cases is rising and 189,582 sufferers worldwide. Every day, about 700 people are diagnosed with a brain tumor.[1] 15 million people are affected by stroke and hemorrhage; of this, 5 million die and another 5 million (2002 estimates) are permanently disabled. Today, over 2,500,000 people around the world have MS.[2]

Currently, the standard lesion pathological classification is based on histological examinations of tissue samples through biopsy. Therefore, radiologists are continuously seeking for greater diagnosis accuracy by the modern medical imaging system. According to the quantitative analysis of computer-aided diagnosis (CAD), it may aid radiologists in the interpretation of the medical images. Recent studies showed that CAD could help to improve the diagnostic accuracy of radiologists, lighten their increasing workload, reduce misinterpretation due to fatigue, or overlooked and improved inter- and intra-reader variability.[3] Manual CAD task is mostly performed by drawing image regions slice-by-slice, limiting the human rater's view, and generating suboptimal outlines with limited consistency across slices. Due to the limitations of manual methods, an automatic CAD framework is crucial for the study of medical phenomena, especially when it involves a large set of images. An automatic segmentation method is desirable because it reduces the workload of human experts and generates fully reproducible segmentations. A computer program also has the advantage of being able to process large amounts of information as typically presented within MR images in a more consistent manner compared to human raters.

Automated identification of brain abnormalities in different medical images demands high accuracy since it deals with life. Furthermore, computer assistance is highly sought in medical institutions because it could improve the results of humans in such a domain where the false negative and positive cases must be at a very low rate. It has been proven that double reading of medical images could lead to better abnormal region detection. However, the cost incurred in

Address for correspondence:
Samir Kumar Bandyopadhyay, JIS University, Kolkata, West Bengal, India. E-mail: 1954samir@gmail.com

double reading is very high; therefore, good software to assist humans in medical institutions is of great interest nowadays.

Computer technology has had a tremendous impact on medical imaging. CAD is a relatively young interdisciplinary technology combining elements of digital image processing with medical image processing. CAD techniques in X-ray, mammogram, and magnetic resonance imaging (MRI) and ultrasound diagnostics yield a great deal of information, which the radiologist has to analyze and evaluate comprehensively in a short time. The interpretation of medical images, however, is still almost exclusively the work of humans, but in the next decades, this change is expected. The computer is used for more image interpretation, and the research area is called CAD.

In this paper, normal and abnormal tissue detection and analysis from brain MRI are proposed.

LITERATURE REVIEW

A large number of approaches have been proposed by various researchers to deal with MRI images. The development of automatic and accurate CAD in characterizing brain lesions is essential, and it remains an open problem.[4] Lesion detection, segmentation, or separation of a particular region of interest is an important process for diagnosis. Computer-aided surgery also requires previous analysis of lesion area inside the brain. This process is a challenging process due to the complexity and large variations in the anatomical structures of human brain tissues, the variety of the possible shapes, locations, and intensities of various types of lesions. Many methods need some preprocessing technique for the improvement of accurate identification of brain abnormalities.

Most of the binarized images fail due to large intensity difference of foreground and background i.e. the black background of MRI image. In region, growing methodologies are not standard methods for validating segmentation; the main problem is the quality of segmentation in the border of the tumor.[5-7] These methods are suitable for the homogeneous tumor but not for heterogeneous tumor. Classification-based segmentation can segment tumor accurately and produce good results for large data set, but undesirable behaviors can occur in a case where a class is underrepresented in training data. Clustered-based segmentation performs very simple, fast and produces good results for the non-noise image, but for noise images, it leads to serious inaccuracy in the segmentation. A neural network-based segmentation performs little better on noise field and no need of assumption of any original data allocation, but the learning process is one of the great disadvantages of it. In spite of several difficulties, an atomization of brain tumor segmentation using a combination of a threshold based, preprocessing, and the level set can overcome the problems and gives efficient and accurate results for brain abnormality detection.[8] Accurate detection is the basis for calculating important features of brain lesion such as size, classification, heterogeneity, and volume of the lesions. The following existing problems are selected from the literature study:

i. The problems for small abnormality detection, undersegmentation, oversegmentation, spurious lesion generation, segmentation two or more abnormality in a brain, false identification, and segmenting abnormality with inhomogeneity during abnormality segmentation.
ii. The subcortical gray matter (GM) is underestimated, a cortical GM is overestimated, and over- and under-segmentation of normal brain tissue and non-brain part are performed by the existing tissues segmentation methodology.
iii. Increased number of structures in the segmentation problem also increases the problem mathematical complexity and a likelihood of misclassified pixels during abnormal and normal tissues segmentation.

To accurate detection and to solve and reduce the existing problems of abnormalities identification from MRI of a brain, there are several steps that need to be done. Thus, proposed framework decomposed into several subworks to correctly identification of abnormality and normal tissues of the brain. From the mentioned problem statements discussed in the summary of this chapter, the specific objectives of this research are as follows: (i) Preprocessing stage: Artifact removal and skull elimination are used to reduce the spurious lesion generation and false detection problem. (ii) Binarization stage: Binarization can be used as an intermediate/preprocessing step of small, multiple, and low intense (or similar intensity with normal tissues) abnormalities detection (e.g. small tumor and MS). (iii) Tissue detection and segmentation: Quantification of normal brain tissues and presence of abnormality (disease such as a tumor, stroke, hemorrhage, and MS) are identified (if any). A brain MRI is normal or abnormal that can be identified during this stage. This stage reduces oversegmentation, undersegmentation, false detection, and misclassification problem of white matter (MW), GM, cerebrospinal fluid (CSF), marrow, and muscle skull. (iv) Abnormality detection and segmentation: This stage is used to accurate detection and quantification, overcome over- and under-segmentation problem, reduce spurious lesion generation, and reduce misclassified pixels during abnormal and normal tissues segmentation of brain abnormalities. (v) Classification of brain tumor: This stage used to classify the five major brain tumors from brain MRI. The preprocessing steps are used to reduce noise and improve the classification accuracy.

Proposed method

MRI is the most frequently used neuroimaging technique for the evaluation and follow-up a review of patients with brain abnormalities for many reasons.[9] It does not use ionizing

radiation such as computed tomography (CT), single-photon emission CT (SPECT), and positron-emission tomography studies.

It is stated that the T1 MRIs have brighter pixels for WM, darker for GM, and almost black for CSF. The T1 images show abnormality with larger intensity value than normal tissue. Therefore, some lesions in the WM areas can look alike GM in T1 images due to the increase of water. Besides, the pixels with muscle tissue appear brighter than for fat. Almost the opposite intensity contrast will be expected in T2 images. The WM is less fluid based. Thus, the pixels with mostly this tissue class will appear white in T1 and dark in T2, which corresponds to high- and low-intensity values, respectively. In the case of GM, it appears darker in T1 images and brighter in the T2 images. Finally, the CSF shows a small peak surrounding large lobe that almost overlaps all the test classes. So it requires segregation of both parts. In proton density (PD) images, MW is brighter than GM, and GM is brighter than CSF. PD, T2, and T1 type of MRI with sarcoma brain abnormality are shown in Figure 1.

The proposed techniques implemented based on brain MRI images consist of normal and abnormal from a real human brain MRI dataset. The dataset used consists of axial, T2, T1, and PD MR brain images. These images were collected from the Harvard Medical School[10] website used for normal and abnormal brain images: (a) Tumors, (b) strokes, (c) hemorrhage, and (d) MS.

Standard simulations from brain web database[11] include parameter setting fixed to 3 modalities (T1, T2, and PD), five slice thicknesses (1, 3, 5, 7, or 9 mm), and defining a volume (x, y, and z). Tissue classes include not only GM, WM, and CSF but also muscle, fat, or skin. The brain model used to generate the simulations can also be employed as ground truth.

A brain tumor is a cluster of abnormal cells due to the loss of normal aging and cell death. It may occur in any person at almost any age. It may even change from one treatment session to the next, but its effects may not be the same for each person. Brain tumors appear at any location and, in different image intensities, can have a variety of shapes and sizes. Brain tumors can be malignant or benign. In this research work, five major tumors such as glioma, meningioma, metastatic adenocarcinoma, metastatic bronchogenic carcinoma, and sarcoma types of tumors are used. Gliomas are a group of tumors that arise in the central nervous system. MRI is currently the method of choice for early detection of a brain tumor in the human brain. Low-grade gliomas and meningiomas are benign tumors. Glioblastoma multiforme is a malignant tumor and may arise anywhere in the brain. Metastatic adenocarcinoma and metastatic bronchogenic carcinoma tumors are the most common type of brain tumors (30% of all) and are usually malignant one. Sarcoma arises nearer to the surrounding structures of the brain. According to the World Health Organization, there are 126 types of different brain tumors, of which many of them arise from structures intimately associated with the brain such as tumors of the covering membranes to the posterior fossa. Figure 2 shows the five major types of tumors in MRI images with arrows.

Stroke

Stroke or cerebrovascular accident is a disease, which affects the vessels that supply blood to the brain. The stroke occurs when a blood vessel either bursts or there is a blockage of the blood vessel. Due to loss of oxygen, nerve cells in the affected brain area are not able to perform basic functions which lead to the death of the brain tissue.[12-14] Stroke leads to serious long-term disability or death. Strokes are mainly classified into two categories: Ischemic stroke or infarct and hemorrhagic stroke, and they require opposite treatments. Figure 3 shows the brain image with acute stroke and subacute stroke with an arrow.

A stroke is caused by a blood clot or leak of blood vessels in the brain. When the brain stops receiving a steady blood flow, it stops working, which can result in similar symptoms as seen in MS, many of them can be chronic.

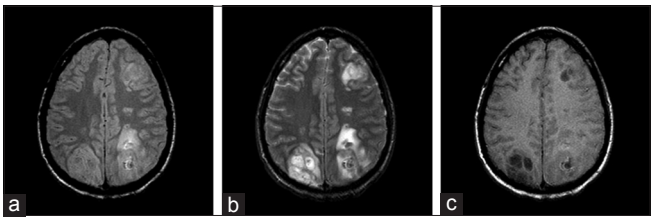

Figure 1: (a) Proton density, (b) T2, and (c) T1 type of magnetic resonance imaging with sarcoma type of brain tumor

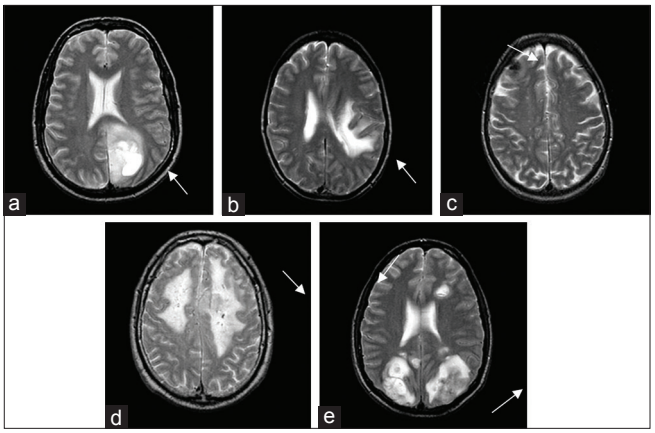

Figure 2: Five major brain tumors in magnetic resonance imaging: (a) Glioma, (b) meningioma, (c) metastatic adenocarcinoma, (d) metastatic bronchogenic carcinoma, and (e) sarcoma

Hemorrhage

Hemorrhage usually refers to head injury, but it is a broader category because it can involve damage to structures other than the brain, such as the scalp and skull. An intracranial hemorrhage is a bleeding process, within the skull. Intracranial bleeding occurs if a blood vessel within the skull bursts or leaks.[15] It can result from non-traumatic causes (as occurs in hemorrhagic stroke) such as a ruptured aneurysm. An intracranial hematoma occurs when a blood vessel ruptures between the skull and brain. Intracerebral hemorrhage, with bleeding into the brain tissue itself, is an intra-axial lesion. Extra-axial lesions include epidural hematoma, subdural hematoma, and subarachnoid hemorrhage. Hematomas or focal lesions are collections of blood in or on the brain that can result from hemorrhage.

Types of intracranial hemorrhage are classified as intra-axial and extra-axial. Intra-axial hemorrhage or intraparenchymal hemorrhage is bleeding within the brain. This category includes intracerebral hemorrhage or bleeding within the brain tissue. It also shows intraventricular hemorrhage and bleeding within the brain's ventricles. Intra-axial hemorrhages are more dangerous and harder to treat than extra-axial bleeds. In extra-axial hemorrhage, bleeding occurs within the skull but outside of the brain tissue. Its three subtypes are epidural hemorrhage, subdural hemorrhage, and subarachnoid hemorrhage. The types of intracranial hematomas are an epidural hematoma, subdural hematoma, intracerebral hematoma, and subarachnoid hemorrhage. Figure 4 shows the cerebral hemorrhage for PD MRI and chronic subdural hematoma for T2 MRI of hemorrhage with an arrow.

MS

MS is a chronic disease that damages the nerves in the spinal cord and brain, as well as the optic nerves. Sclerosis means scarring, and people with MS develop multiple areas of scar tissue in response to the nerve damage.[16] MS is the result of damage to myelin, a protective sheath surrounding nerve fibers of the central nervous system. When myelin is damaged, this interferes with messages between the brain and other parts of the body. Symptoms vary widely and include blurred vision, weak limbs, tingling sensations, unsteadiness, and fatigue. For some people, MS is characterized by periods of relapse and remission, while for others, it has a progressive pattern. For everyone, it makes life unpredictable. Contrast is the means by which it is possible to distinguish among soft tissue types owing to differences in observed MRI signal intensities. For example, in musculoskeletal imaging, there are differences among cartilage, bone, and synovial fluid. In neuroimaging, there are differences between white and GM. The fundamental parameters that affect tissue contrast are the T1 and T2 values, PD, tissue susceptibility, and dynamics. MS is one of the most common diseases of the central nervous system. Figure 5 shows the MS lesions with arrows.

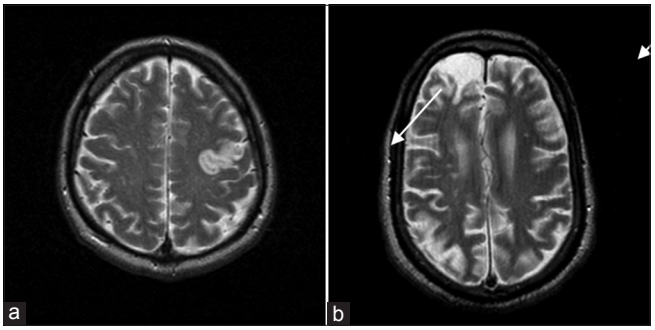

Figure 3: Magnetic resonance imaging of brain stroke images: (a) Speech arrest due to acute stroke (b) loss of sensation due to subacute stroke

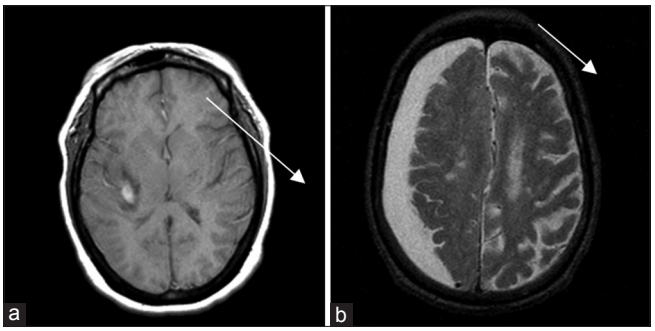

Figure 4: Magnetic resonance imaging of brain hemorrhage images; (a) cerebral hemorrhage, (b) chronic subdural hematoma

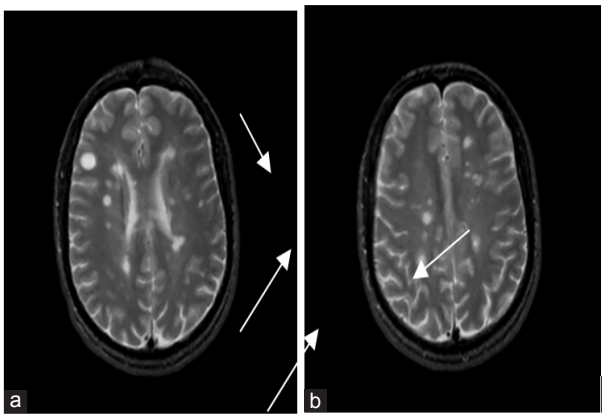

Figure 5: (a and b) are the magnetic resonance imaging with MS lesions in the brain

Performance measurement

Artifact removal technique can remove the artifacts if any artifacts present in the brain MRI. Proposed method is tested on a large dataset and produces excellent results except for connected artifact with the original brain portion image. The accuracy is used to evaluate the performance of the proposed methods for finding errors such as relative area error (RAE or RE), kappa index (KI), Jaccard index

(JI), correct detection ratio (CDR) and false detection ratio (FDR). A critical problem faced in performance evaluation of artifacts and skull removal method is the lack of a gold standard. Here, we use ground truth suggested by a radiologist for the comparison with the automated method and measure their performance with the help of RE, KI, JI, CDR, and FDR. Segmented area of the brain and the brain without skull using proposed method with 341 × 341 image size are shown in Table 1.

A higher value of CDR and lower value of FDR mean the good results. A method could be better when JI and CDR value is more and less value of FDR so that the best method would be the maximum value of JI and CDR and the minimum value of FDR. Area of reference segmentation and the intersection between the reference and proposed method are also displayed in Table 1. Intersection pixels determine the exact number of pixel matches between automated segmented and manual (reference) segmented.

In medical imaging, low error is required as much as possible because increased error reflects the wrong diagnosis. Removing artifacts and skull by keeping all necessary information (soft tissues of the brain) is the key goal of preprocessing. The relative area error (RE) and FDR for the brain with a skull (artifact removal) and without skull (artifacts and skull removal) are shown in Table 2.

The usefulness of pre-processing method also depends on correct segmentation or preprocessing. The values of different accuracy metrics KI, JI, and CDR for preprocessing have been shown in Table 3.

In the visual context, proposed method gives optimized results in almost every respect, but it may be biased without its performance evaluation. The performance evaluation of image segmentation methods is a challenge for medical image analysis system because truthfulness of preprocessing is an important factor for the post-processing technique of several automated systems as

Table 1: Area of without artifacts and brain without skull using proposed and manual segmentation with their intersection

Image sequence	Without artifacts			Brain without skull		
	Automated	Manual	Intersection	Automated	Manual	Intersection
1	44246	45148	44232	30423	31062	30375
2	43672	44484	43649	28210	29125	28189
3	44135	44492	44125	30156	30483	30126
4	43581	44007	43389	29479	30282	29442
5	45278	45392	45198	30281	30933	30241
6	44288	45183	44206	29940	30426	29937
7	43218	44090	43183	28943	29471	28941
8	43826	44164	43820	29781	30282	29768
9	43002	44083	42960	29162	30001	29153
10	43539	44006	43502	29872	31206	29866

Table 2: RE and FDR performance metric

Image sequence	RE		FDR	
	Without artifacts	Brain without skull	Without artifacts	Brain without skull
1	1.99	2.05	0.03	0.15
2	1.82	3.14	0.05	0.07
3	0.80	1.07	0.02	0.09
4	0.96	2.65	0.43	0.12
5	0.25	2.10	0.17	0.12
6	1.98	1.59	0.18	0.01
7	1.97	1.79	0.07	0.01
8	0.76	1.65	0.01	0.04
9	2.45	2.79	0.09	0.03
10	1.06	4.27	0.08	0.02

FDR: False detection ratio

Table 3: KI, JI, and CDR performance metric

Image sequence	KI		JI		CDR	
	Without artifacts	Brain without skull	Without artifacts	Brain without skull	Without artifacts	Brain without skull
1	98.96	98.80	97.94	97.64	97.97	97.79
2	99.03	98.33	98.07	96.72	98.12	96.78
3	99.57	99.36	99.15	98.73	99.18	98.82
4	99.08	98.53	98.16	97.11	98.60	97.22
5	99.68	98.80	99.39	97.64	99.57	97.76
6	98.82	99.18	97.66	98.38	97.83	98.39
7	98.92	99.09	97.86	98.19	97.94	98.20
8	99.60	99.12	99.21	98.26	99.22	98.30
9	98.66	98.55	97.36	97.14	97.45	97.17
10	99.38	97.80	98.77	95.69	98.85	95.71

KI: Kappa index, JI: Jaccard index, CDR: Correct detection ratio

Table 4: Segmented area and evaluation metric for MRI of the brain

Image number	AB	MB	TP	FP	FN
1	21216	21346	21123	0093	223
2	8580	8497	8440	0140	057
3	43059	42006	41956	1103	050
4	50961	50423	50396	0565	027
5	13737	13445	13107	0630	338
6	22971	22678	22587	0384	091
7	27945	28009	27905	0040	104
8	25953	25848	25804	0149	044
9	23562	23156	23096	0466	060
10	21975	21326	21067	0908	259
11	24568	24857	24547	0021	310
12	29757	29896	29724	0033	172
13	24678	24642	23784	0894	858
14	19756	20864	19704	0052	1160
15	22749	22138	22135	0614	003

MRI: Magnetic resonance imaging

Table 5: Performance metric for MRI of brain based on Table 4

Image number	RE (%)	KI (%)	JI (%)	CD (%)	FD (%)
1	0.609	99.25	98.52	98.95	0.435
2	0.976	98.84	97.71	99.32	1.647
3	2.506	98.64	97.32	99.88	2.625
4	1.066	99.41	98.83	99.94	1.120
5	2.171	96.43	93.12	97.48	4.685
6	1.292	98.95	97.94	99.59	1.693
7	0.228	99.74	99.48	99.62	0.142
8	0.406	99.62	99.25	99.82	0.576
9	1.753	98.87	97.77	99.74	2.012
10	3.043	97.30	94.75	98.78	4.257
11	1.162	99.33	98.66	98.75	0.084
12	0.464	99.65	99.31	99.42	0.110
13	0.146	96.44	93.13	96.51	3.627
14	5.310	97.01	94.20	94.44	0.249
15	2.759	98.62	97.28	99.98	2.773

KI: Kappa index, JI: Jaccard index

it grants to the degree to which the preprocessing (binarization) results agree with the ground truth. Manual segmentation normally gives the finest and most dependable outcome based on recognizing structures for a meticulous clinical data. Due to the shortcoming of computerized ground truth creation method, the quantitative estimation of a binarization method is complicated to achieve. An alternative approach is to use manual-binarization results as the ground truth by a specialist. The accuracy measures used to evaluate the performance of the proposed methods are the RE, KI, JI, CD, and FD.

In Table 4, segmented area with a manual and proposed method with their intersection region is shown. Table 5 shows different performance evaluation metric derived from Table 4.

From Table 5, we can find average value of RE (%) = 1.59, average of KI(%) = 98.54, average of JI(%) = 97.15, average of CD(%) = 98.81, and average of FD (%) = 1.73. Proposed binarization technique is used as a key intermediate of MS lesion segmentation.

Proposed method has been tested with a couple of MRI of brain images.[10,11] Brain web is a dataset which provides brain MRI for different acquisition modalities, and it grounds truth segmentation such as T1, T2, and PD.[10,11] The outputs of different steps of proposed methodology with almost perfect segmentation for transverse type MRI are shown in Figure 6. It is noted that all parameters that appear in the method are set to fixed values, so all results shown here have been achieved with the same parameters.

The proposed method is an automatic, multi-scale, brain tissue segmentation algorithm that reaches to very good acceptable results. The proposed methodology can detect the abnormality in the brain lesion if any. A level set based minimization scheme is used in proposed methods based on varying segmentation model through iterative concepts. It changes the speed of finding the level set. Normally the popular level set framework has only been used for two-region segmentation or segmentation with a fixed number of regions. Moreover, maintaining hierarchical structure based on sharp peak provides good initializations, so the method has not any leakage and less sensitive to local minima and maxima than comparable methods. The performance of the proposed model with the existing well-known method shows that proposed method gives better accurate and stable results for transverse, coronal, and sagittal MRI image. The proposed method removes over and under-segmentation problem and improves segmentation accuracy compared to other gold standard and recent methods. All advantages of the level set framework are preserved, while its main problem has been solved using the proposed method.

An image of a normal brain shows a distribution of GM that appears clear in the texture-like fissures, while an abnormal brain has a shape which appears brighter than the normal GM. Abnormal regions of the brain differ in characteristics than the normal brain, but the diversity of characteristics is notable when compared to any other organ for T1, T2, and PD type of MRI images. Thus, accurate segmentation is very important and considerable attention has been given to achieve the same. For brain hemorrhage segmentation, several steps have been proposed, and details are shown in Figure 7.

The output of the segmented abnormal regions and location of the abnormal regions play an important role in the diagnosis of different types of tumor and treatment planning. The proposed method gives very good results on tumor segmentation of different MR of brain images. Our proposed methods show the top, bottom, left, and right position of the abnormal regions with the prominent centroid of the abnormal regions. It improve diagnosis quality. Figure 8 shows that the output of the proposed methods describes earlier test on image standard dataset.[10-12]

Here, the segmented abnormal regions and location of the abnormal regions are clearly visible in the output as shown in Figure 8. Proposed methodology tested on both normal and abnormal tumor images, and segmentation reduces false detection for normal regions image. Another two MRI of the brain images with segmented abnormal lesion and location of the abnormal lesion with heterogeneous natures are shown in Figure 9.

Segmentation results of four major types of tumor sarcoma, meningioma, metastatic bronchogenic carcinoma, and glioma have been shown in Figure 10. The problem of multiple tumor segmentation, heterogeneous tumor segmentation, and

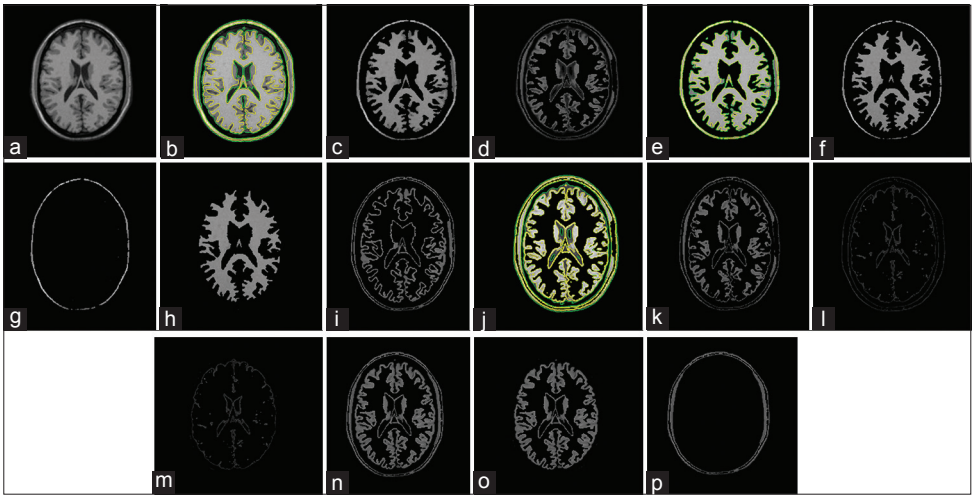

Figure 6: Results of segmented tissues using proposed method where (a) is inputted magnetic resonance imaging, (b) after 3-phase level set, (c) segmented region 1, (d) segmented region 2, (e) repeating level set, (f) segmented part1 from "(e)" (g) is marrow, (h) is WM, (i) segmented part 2 from "(e)", (j) repeating segmentation on "(d)", (k) segmented region 1 of "(j)", (l) segmented region 2 of "(j)" (m) is cerebrospinal fluid, (n) combination of "(k)" and "(i)" (o) is gray matter, and (p) is muscles skin

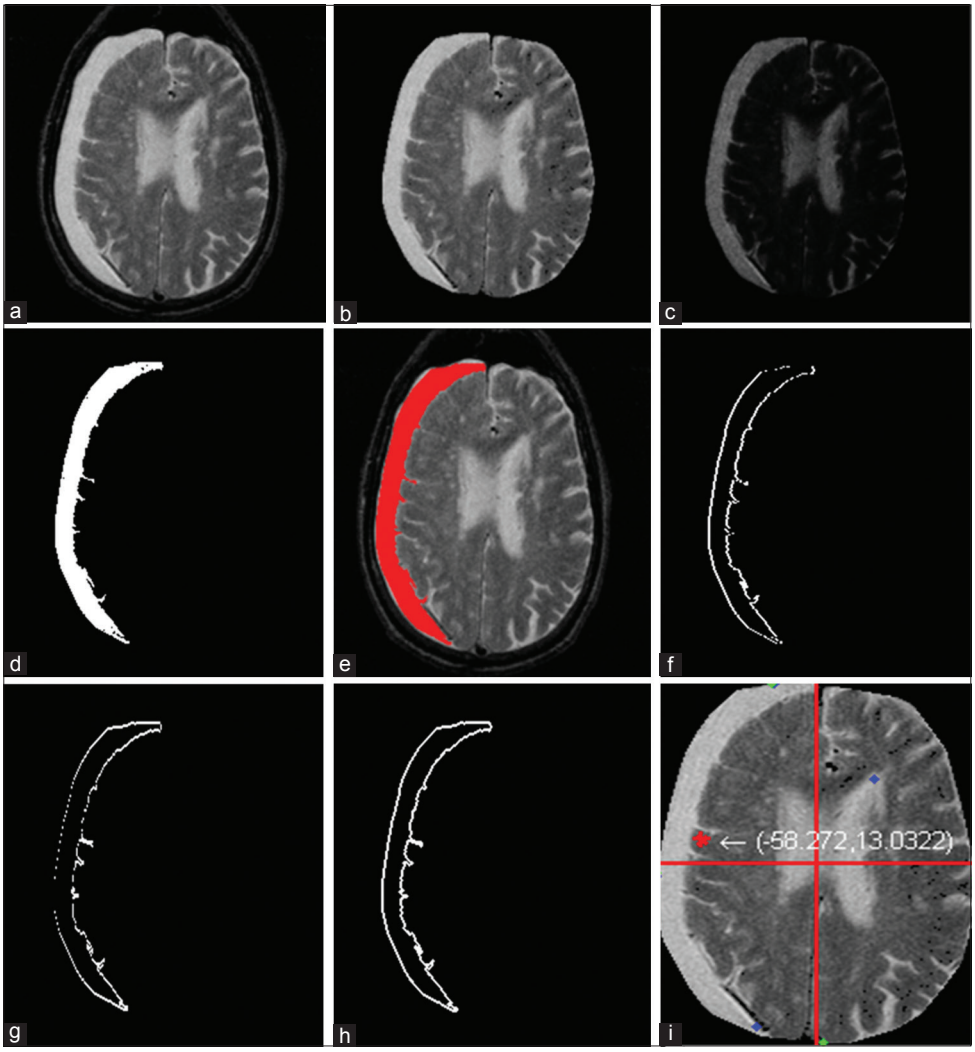

Figure 7: Hemorrhage segmentation results. (a) Input magnetic resonance imaging of the brain, (b) applying artifacts and skull removal, (c) after gamma transformation, (d) segmented abnormal portion, (e) abnormal portion indicated by red marks, (f) horizontal contour, (g) vertical contour, (h) contour of abnormal region, (i) localization of abnormal region

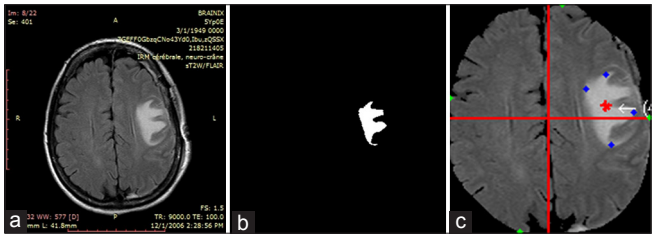

Figure 8: Results on tumor image. (a) Is input magnetic resonance of brain image, (b) is the segmented abnormal region, (c) is the position and centroid of the abnormal lesion

false detection has been solved using proposed segmentation. From the segmented results it clearly shows that proposed method can segment different types of the tumor with reduced error with high accuracy visually.

Figure 10: Four major types of tumor sarcoma, meningioma, metastatic bronchogenic carcinoma, and glioma. (b and d) are the segmented results for input image (a and c); where 1 for sarcoma, 2 for metastatic bronchogenic carcinoma, 3 for meningioma, and 4 for glioma

Another problem mentioned in problem definition related to heterogeneous tumor segmentation has been solved using our proposed method. Proposed methods able to segment heterogeneous lesion. It also helps to detect lesion identification of tumor region and dead cell. Heterogeneous tumor segmentation with glioma grade-I and their heterogeneous structure segmentation by KMeans clustering[10] are shown in Figure 11.

Automated MS lesion detection and segmentation are complex and challenging. The progression of the MS lesions shows considerable variability, and it presents temporal changes in shape, location, and the area between patients and even for the same patient. Hence, correct segmentation

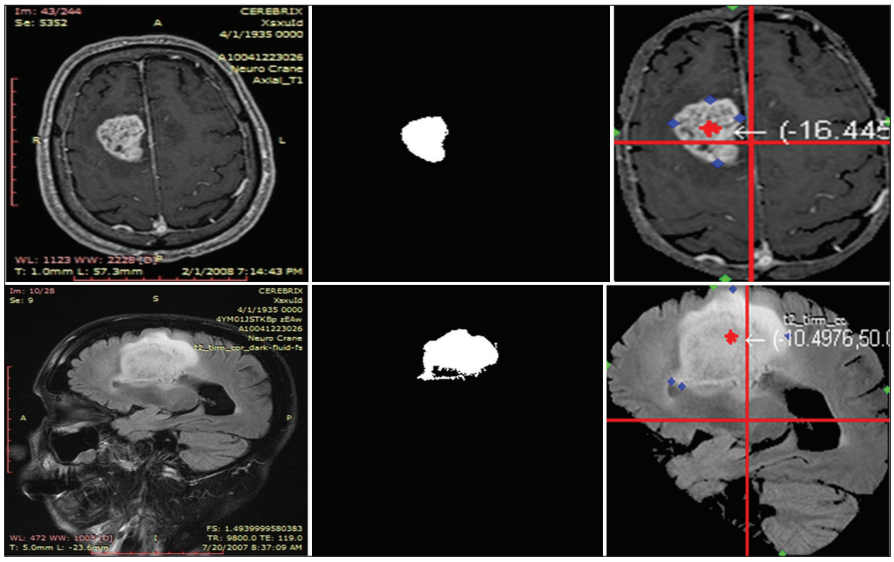

Figure 9: Results of tumor images with heterogeneous nature. (a1, a2) are input magnetic resonance of brain images and (b1, b2) are the segmented abnormal lesion; (c1, c2) are the position and centroid of the abnormal lesions

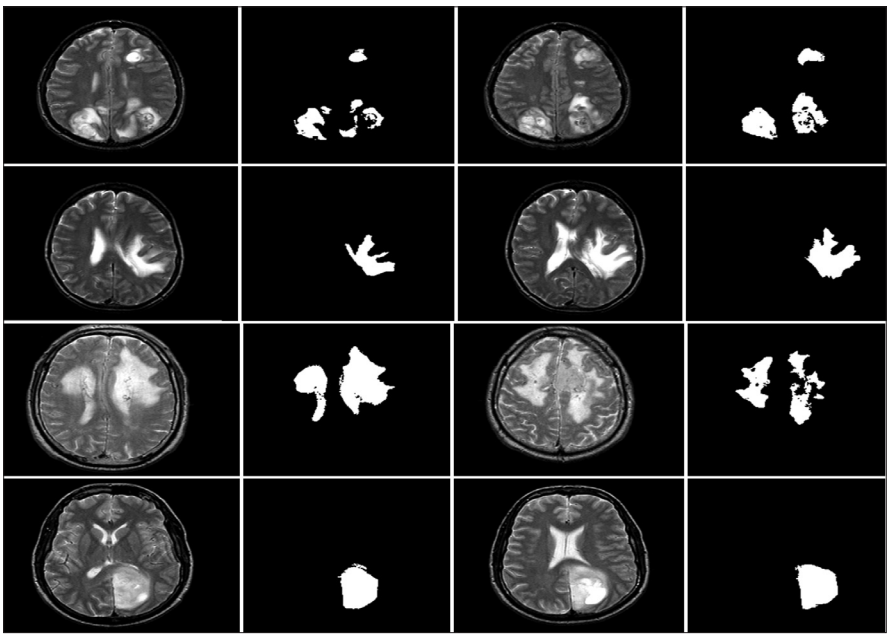

Figure 10: Four major types of tumor sarcoma, meningioma, metastatic bronchogenic carcinoma, and glioma. (b and d) are the segmented results for input image (a and c); where 1 for sarcoma, 2 for metastatic bronchogenic carcinoma, 3 for meningioma, and 4 for glioma

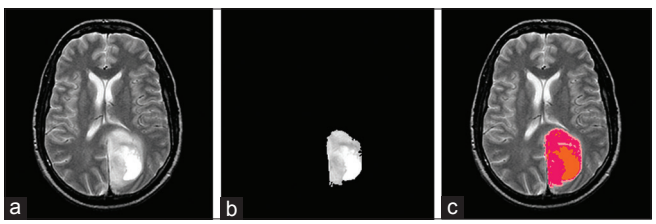

Figure 11: Heterogeneity of brain tumor. (a) is the input glioma Grade-I, (b) is the segmented results, (c) showing its heterogeneity

with its localization is very important, and the results of our method are shown in Figure 12.

More clear visions of different lesions with their position have been shown in Figure 13. Intersections of the red line indicate the midpoint. Green dots in the top, left, bottom, and right are the corresponding extreme ends of the brain. Blue dots in the top, left, bottom, and right are the highest, left, right, and lowest pixels of segmented MS lesion. From those set of positions, we measure the distances.

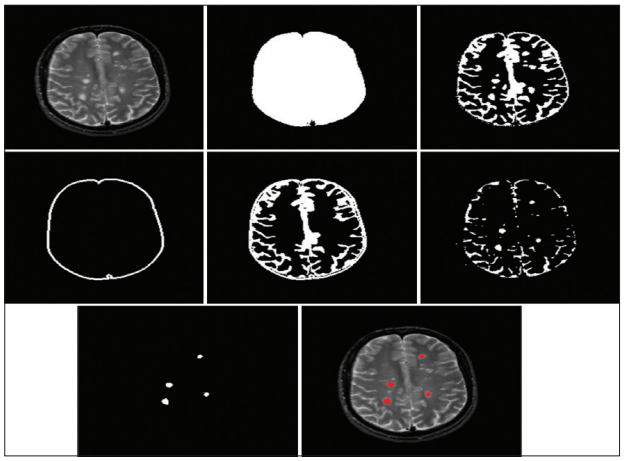

Figure 12: Result of MS lesions segmentation. (a) Input brain image, (b) binary image after skull removal from (a), (c) CSF segmentation from without skull image, (d) combination of horizontal and vertical contour from (b), (e) background generation from (c) and (d), (f) output after binarization, (g) segmented MS lesions from (f) and (e), and (h) finally, MS lesions are shown as red color in inputted brain image (a)

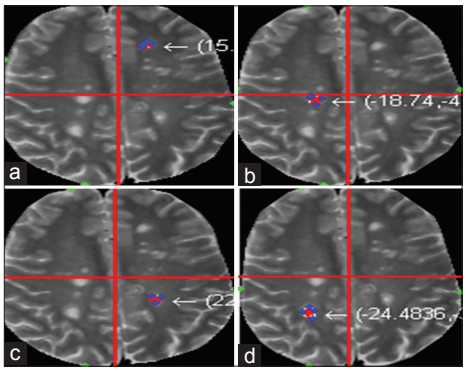

Figure 13: Locations of four magnetic resonance lesions are shown in (a) top right lobe, (b) near middle left lobe, (c) bottom right lobe, and (d) bottom left lobe with red color

The methodology has been implemented and tested in MATLAB software (version R2009a). The training dataset is generated from image database.[10-12] After training, it is tested against the testing dataset generated from the input slice. The predicted class is compared to the actual class label to measure the efficiency of the classifier. The testing of this methodology was carried on a personal computer with an Intel cour2duo processor with 2.50 GHz clock speed and 8 GB RAM.

In this processes, the images are normalized to the feature vector containing 12 features which are extracted from the slices. Each of the feature vector forms an input tuple to the classifier. This vector is generated for 20 input slices as shown in Figure 14.

CONCLUSIONS

The classifier obtained 96.34% accuracy on Harvard benchmark dataset for both contrast and non-contrast images. Feature extraction involves simplifying a number of resources required to describe a large set of data accurately. When performing analysis of complex data, one of the major problems stems from the number of variables is involved. Analysis with a large number of variables requires a large amount of memory and computation power or a classification algorithm which overfits the training sample and also generalizes successfully to new samples. ANFIS helps to classify models by enhancing generalization capability. Automation of a model for computing an estimate of the type of tumor is verified by a radiologist, and a simultaneous measure of the quality of each phase is required to readily assess the automated image classification and segmentation algorithm performance. The proposed system can help the physicians to identify the type of brain tumors for further treatment.

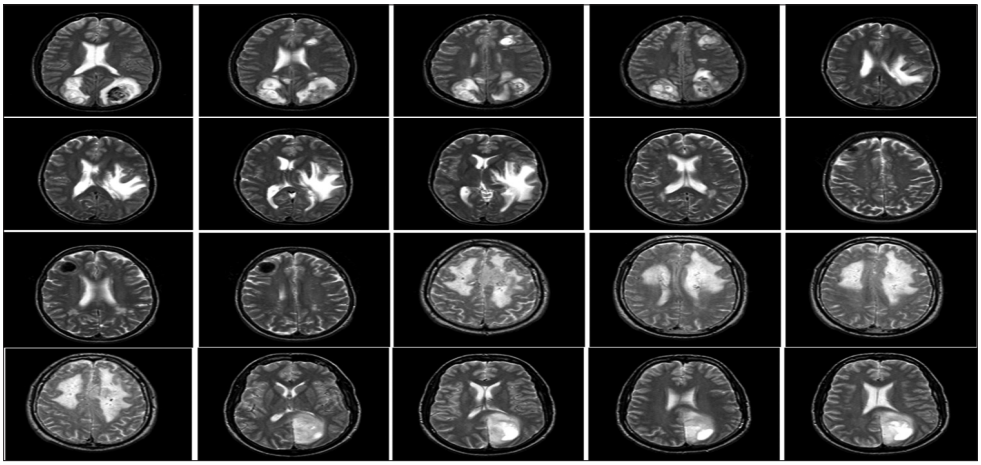

Figure 14: 20 input slices passed through the normalization and feature extraction processes for classification. After classification, we found that slices I1–I4 are Type 1 (Sarcoma), slices I5–I8 are Type 2 (meningioma), slices I9–I12 are Type 3 (metastatic adenocarcinoma), slices I13–I16 are Type 4 (metastatic bronchogenic carcinoma), and slices I17–I20 are Type 5 (Glioma)

REFERENCES

1. WHO-International Agency for Research on Cancer. GLOBOCAN. Estimated Cancer Incidence, Mortality and Prevalence Worldwide; 2012. Available from: http://www.globocan.iarc.fr/Default.aspx. [Last retrieved on 2016 Aug].
2. The Multiple Sclerosis International Federation. (n.d.). Multiple Sclerosis in Children. from: https://www.msif.org/. [Last retrieved on 2016 Feb].
3. EI Dahshan ES, Hosny T, Salem AB. Hybrid intelligent techniques for MRI brain images classification. Digit Signal Process 2010;20:433-41.
4. Sezgin M, Sankur B. Survey over image thresholding techniques and quantitative performance evaluation. J Electron Imaging 2004;13:146-65.
5. Otsu N. A threshold selection method from gray level histograms. IEEE Trans Syst Man Cybern SMC 1979;9:62-6.
6. Vidyarthi A, Mittal N. A Hybrid Model for Extraction of Brain Tumor in MR Images. International Conference on Signal Processing and Communication (ICSC), IEEE; 2014 p. 202-206.
7. Kaur A. An Automatic Brain Tumor Extraction System using Different Segmentation Methods. International Conference on Communication, Information and Computing Technology, IEEE 2016. pp. 178-91.
8. Bernsen J. Dynamic Thresholding of Gray Level Images. In: ICPR'86: Proceedings of the International Conference on Pattern Recognition; 1986. p. 1251-5.
9. Ricci PE, Dungan DH. Imaging of low- and intermediate-grade gliomas. Semin Radiat Oncol 2001;11:103-12.
10. Johnson KA, Becker JA. The Whole Brain Atlas; 1999. Available from: http://www.med.harvard.edu/aanlib/. [Last retrieved on 2016].
11. .Cocosco CA, Kollokian V, Evans AC, Kwan RK, Pike GB, Collins DL, *et al.* (1996). BrainWeb: Simulated Brain Database. Available from: http://www.brainweb.bic.mni.mcgill.ca/brainweb/. [Last retrieved on 2016].
12. Easy Analytic Software, Inc. The EASI MRI Reports: EASI Media Mark Propensity Reports. (n.d.). Availale fom: https://www.easidemographics.com/Cgi-bin/DbMri.asp. [Last retrieved on 2016 Apr 08].
13. About Brain Tumors: A primer for patients and caregivers. Am Brain Tumor Assoc 2015;2015:1-84. Available from: http://www.abta.org/secure/about-brain-tumors-a-primer.pdf. [Last retrieved on 2016].
14. Maier O, Schröder C, Forkert ND, Martinetz T, Handels H. Classifiers for ischemic stroke lesion segmentation: A comparison study. PLoS one 2015;10:1-16.
15. Siddiqui FM, Bekker SV, Qureshi AI. Neuroimaging of hemorrhage and vascular defects. Neurotherapeutics 2011;8:28-38.
16. Messina S, Patti F. Gray matters in multiple sclerosis: Cognitive impairment and structural MRI. Mult Scler Int 2014;2014:609694.

How to cite this article: Roy S, Bandyopadhyay SK. Description of Different Phases of Brain Tumor Classification. J Clin Res Radiol 2018;1(1):1-11.